Applied Surface Science xxx (2013) xxx–xxx

Contents lists available at SciVerse ScienceDirect

Applied Surface Science

journal homepage: www.elsevier.com/locate/apsusc

Microstructure and corrosion behavior of TiC/Ti(CN)/TiN multilayer CVD coatings on high strength steels

Jin Zhang, Qi Xue*, Songxia Li

School of Materials Science and Engineering, Southwest Petroleum University, 610500 Chengdu, PR China

ARTICLE INFO

Article history:
Received 23 October 2012
Received in revised form 2 May 2013
Accepted 2 May 2013
Available online xxx

Keywords:
TiC/Ti(CN)/TiN
Multilayer coatings
Hydrogen sulfide corrosion
High-strength steels

ABSTRACT

Titanium carbide/titanium carbonitride/titanium nitride (TiC/Ti(CN)/TiN) multilayer coatings are prepared on the surface of three high-strength steels (35CrMo, 42CrMo, and 40CrNiMo) by chemical vapor deposition method. The fracture morphology, elemental distribution, phase composition, microhardness, and adhesion of the multilayer film are analyzed. The hydrogen sulfide stress corrosion resistance of the coating is evaluated by the National Association of Corrosion Engineers saturated hydrogen sulfide solution immersion test. A test simulating the environment of the natural gas wells with high temperature and pressure in Luojiazhai in Sichuan is also performed. The results show that the multilayer coatings have dense structures, ~11 μm thickness, 24.5 ± 2.0 GPa nano-hardness, and ~70 N adhesion. The corrosion sample also shows no brittle failure induced by stress corrosion after treatment with the coating. Gravimetric analysis shows that the deposition of TiC/Ti(CN)/TiN multilayer coatings results in a corrosion rate reduction of at least 50 times compared with the high-strength steel substrate. A preliminary analysis on this phenomenon is conducted.

1. Introduction

Given the high-sulfur, high-temperature, and high-pressure environment of sour oil and natural gas wells, their exploration and development require special drilling tools. These tools must be made of high-strength steels (e.g., 35CrMo), which are characterized by a high carbon content, ≥1600 MPa tensile strength, and ≥HRC35(HV329) hardness during use [1]. In oil and gas fields, the high content of hydrogen sulfide and other acidic corrosive media, high temperature, and high pressure cause a hydrogen evolution reaction to occur between the wet hydrogen sulfide and the material surface. This reaction produces hydrogen atoms, which make contact with the material and induce cracking, known as hydrogen embrittlement [2,3]. When the hardness of steel parts is higher than HRC22(HV237), hydrogen-induced stress corrosion cracking is extremely sensitive; when the hardness is over HRC27(HV268), stress corrosion is inevitable [4]. Hydrogen embrittlement always inflicts partial or even overall structural damage to drilling tools, such as blowout preventer, packer, and so on. This damage is hardly perceptible in advance.

To prevent the destruction of high-strength steel caused by hydrogen sulfide corrosion, oil fields use high-cost nickel-based and titanium alloy corrosion-resistant materials to make tools [5]. Traditional protective methods such as the addition of a corrosion inhibitor and desulfurization do not significantly prevent hydrogen sulfide corrosion.

Hard ceramic coatings such as titanium nitride (TiN), titanium carbide (TiC), and titanium carbonitride (Ti(CN)) are widely used in industrial application [6]. Each layer provides an attractive feature that provides superior coating properties. TiN improves the service life of tools working at high speeds by tailoring surface properties, such as decreasing the coefficient of friction and improving wear resistance. TiC increases coating hardness [7–9]. Ti(CN) coating is a very interesting coating because it combines the high hardness of TiC phases and the high toughness of TiN phases [10–12]. Given that Ti(CN) has a thermal expansion coefficient similar to those of steel substrates, Ti(CN) can well alleviate the internal stress between coating and substrate. Ti(CN) has a hydrogen barrier layer effect as well [13,14], so it can be considered as a protective material against hydrogen sulfide corrosion on the surface of high-strength steels. Compared with a single-layer coating, more interfaces exist between multilayer films, which decrease the number of pores and defects as well as enhance the ability to resist crack extension [15–17]. Thus, multilayer coatings have higher hardness and corrosion resistance, which can further improve the mechanics and corrosion resistance of the base.

In this paper, CVD is used to deposit multilayer titanium carbide (TiC)/Ti(CN)/titanium nitride (TiN) ceramic coatings on the surface of 35CrMo, 42CrMo, and 40CrNiMo steels. The fracture morphology, elemental distribution, phase composition, nano-hardness,

* Corresponding author. Tel.: +86 28 83037438; fax: +86 28 83037406.
E-mail address: xqswpu@gmail.com (Q. Xue).

0169-4332/$ – see front matter © 2013 Elsevier B.V. All rights reserved.
http://dx.doi.org/10.1016/j.apsusc.2013.05.037

Table 1
Chemical composition of the three steel substrates (wt.%).

Substrate	C	Si	Mn	Cr	Mo	Ni
35CrMo	0.32–0.4	0.17–0.37	0.4–0.7	0.8–1.1	0.15–0.25	–
42CrMo	0.38–0.45	0.17–0.37	0.5–0.8	0.9–1.2	0.15–0.25	–
40CrNiMo	0.37–0.44	0.17–0.37	0.5–0.8	0.6–0.9	0.15–0.25	1.25–1.65

and adhesion of the coatings, as well as the anti-hydrogen sulfide corrosion of the composite materials are studied.

2. Experimental

2.1. Base material for the test

The chemical composition of the three high-strength steels used in the test is shown in Table 1.

2.2. Preparation of the multilayer coatings

Oil was removed from the three high-strength steel substrates, and then they were cleaned ultrasonically with absolute alcohol. After sand blasting (0.4 MPa), the steel substrates were placed in a self-built chemical vapor reactor and vacuum extraction was performed at 0.005 MPa. Hydrogen was fed into the reactor, which was heated to 950 °C and maintained at this temperature for 30 min. Reaction gases were then fed into the reactor to coat the steel samples. For the TiC film, the following gases were fed: H_2 at 0.7 mol/min, CH_4 at 0.075 mol/min, and $TiCl_4$ evaporated gas at 0.03 mol/min; the total coating time was 35 min. For the Ti(CN) film, the following gases were fed: N_2 at 0.55 mol/min, CH_4 at 0.06 mol/min, $TiCl_4$ evaporated gas at 0.04 mol/min; the total coating time was 40 min. For the TiN film, the following gases were fed: N_2 at 0.55 mol/min and $TiCl_4$ evaporated gas at 0.04 mol/min; the total coating time was 40 min. The coated steel samples were then subjected to 870 °C vacuum oil quenching and tempering at a low temperature (180 °C).

2.3. Corrosion test

The saturated hydrogen sulfide corrosion immersion test and the test simulating the environment of acidic gas wells with high temperature and pressure in Luojiazhai in Sichuan were both conducted in the Acidic Oil and Gas Field Material Corrosion Detection and Evaluation Center of the Sichuan Petroleum Administration [18]. The tests were performed as follows.

Samples with and without CVD (50 mm × 15 mm × 4 mm) were placed in the simulated environment of acidic gas wells with high temperature and pressure in Luojiazhai, Sichuan for immersion. The test conditions were as follows: total gas pressure, 32 MPa; H_2S gas partial pressure, 3.4 MPa; and CO_2 gas partial pressure, 3.1 MPa. The samples were completely immersed in a container with 20,000 ppm Cl^- solution at 80 °C for 96 h of corrosion. After corrosion, the samples were subjected to gravimetric analysis to determine the corrosion rate.

The test bars with and without CVD were immersed in the National Association of Corrosion Engineers (NACE) environment (NACE TM0177-A standard) at the ambient pressure and room temperature (25 °C). The size of the test bars is shown in Fig. 1. The pH of the solution was 3.12 and the immersion time was 168 h. After immersion, the test bars were subjected to a standard tensile test within 24 h to observe the fracture morphology, measure the reduction of the cross-sectional area, and evaluate the hydrogen-induced stress corrosion cracking condition of the substrates and the coated samples in the saturated hydrogen sulfide environment.

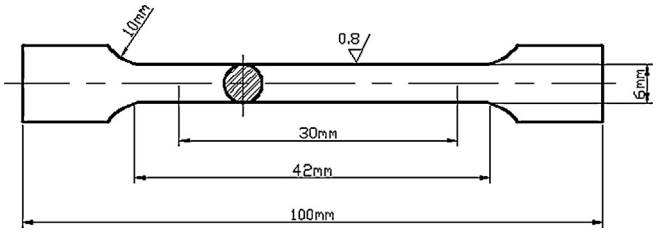

Fig. 1. Dimensions of the tensile test bars.

The distribution of the elements along the coating thickness was analyzed by using X-ray spectroscopy (EDS). The cross-sectional and fracture morphologies after corrosion were observed by scanning electron microscopy (SEM). The phase composition and structure of the samples after corrosion were analyzed by X-ray diffraction (XRD).

The nano-hardness of the coating was tested with a computer-controlled nano-indenter (Aligent G200, American) using a Vickers indenter and continuously applied load. A two-step penetration method was used to measure the nano-hardness of the coatings. A maximum load with a holding time of 10 s was used to examine the hardness of the coatings.

To diminish the effect of films and substrate, a smaller load of 5 mN was used to measure the nano-hardness of the coatings. The Vickers indentation depth was <10% of the coating thickness. The Vickers hardness was computed from the load/unload displacement curves by adopting the Oliver and Pharr formula. The hardness value was the average of 10 measurements. The adhesion between the film and base was examined with a MFT-4000 multifunction surface property tester. At least six replicates were performed for each sample, and the average values were recorded.

3. Results and discussion

3.1. Cross-sectional morphology of the coatings and elemental distribution

Fig. 2 shows the SEM image of the TiC/Ti(CN)/TiN multilayer film growing on the 35CrMo steel surface by CVD. The total thickness of the ceramic coating is about 11 μm, and the film layer is relatively dense. The layers are closely integrated, and the interface between the film and substrate is flat without pores and defects, which indicate good interfacial bonding properties. These observations are further confirmed by a subsequent scratch test.

Fig. 3 shows the elemental distribution diagram of the fracture surface of the coatings scanned from the top of the coating to the steel substrate. The coating layer includes Ti, C, N, and a few Fe without any other impurity elements. The TiC layer is closest to the substrate, the TiN layer is the outermost layer, and the Ti(CN) layer is the transition layer in the middle. This multilayer structure effectively relieves the internal stress between the coatings as well as between the coating and substrate, thereby improving the coating properties [19,20].

Please cite this article in press as: J. Zhang, et al., Microstructure and corrosion behavior of TiC/Ti(CN)/TiN multilayer CVD coatings on high strength steels, Appl. Surf. Sci. (2013), http://dx.doi.org/10.1016/j.apsusc.2013.05.037

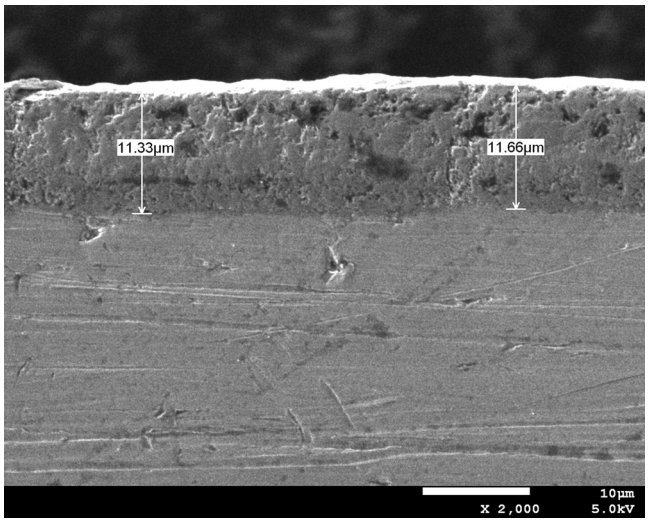

Fig. 2. Cross-sectional SEM image of TiC/Ti(CN)/TiN coatings.

3.2. Nano-hardness and adhesion of the coatings

The multilayer coating surface deposited onto different steel substrates was cleaned with acetone. The average nano-hardness of the coatings is approximately 24.5 ± 2.0 GPa (2500 HV), which is five times higher than that of the substrate (4.7 ± 1.3 GPa; 485 HV).

Fig. 4 shows the surface scratch test curve and as well as the morphology of the adhesion between the multilayer coatings and 35CrMo steel substrate. Two modes of acoustic emission and friction are observed [21]. Analysis of the trend of the two curves reveals that the adhesion between the multilayer coating and steel substrate is almost 70 N, which indicates high adhesion between the steel and ceramic coating. This finding can be attributed to the similarity of the structure and thermal parameter of TiC to those of the steel substrate. Thus, the compatibility of both sides of the interface is good. The gradient transition structure of TiC/Ti(CN)/TiN

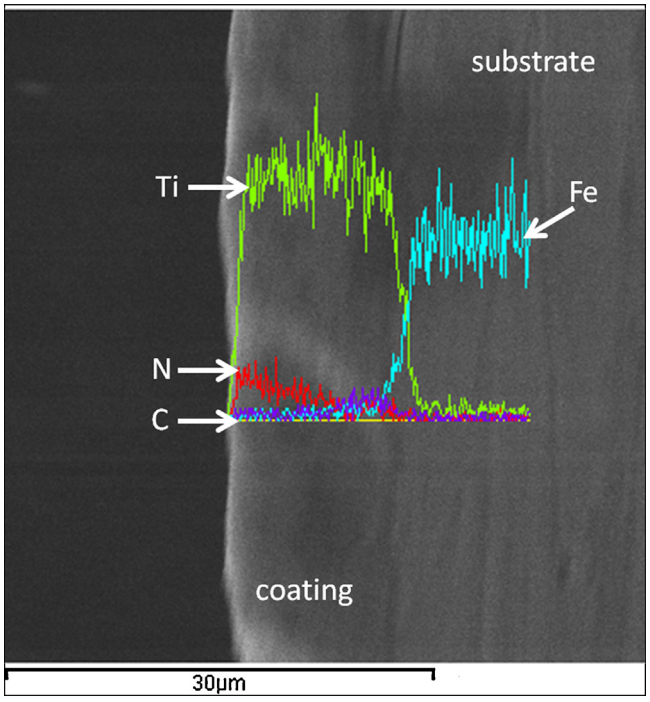

Fig. 3. EDS spectrum of fracture element distribution.

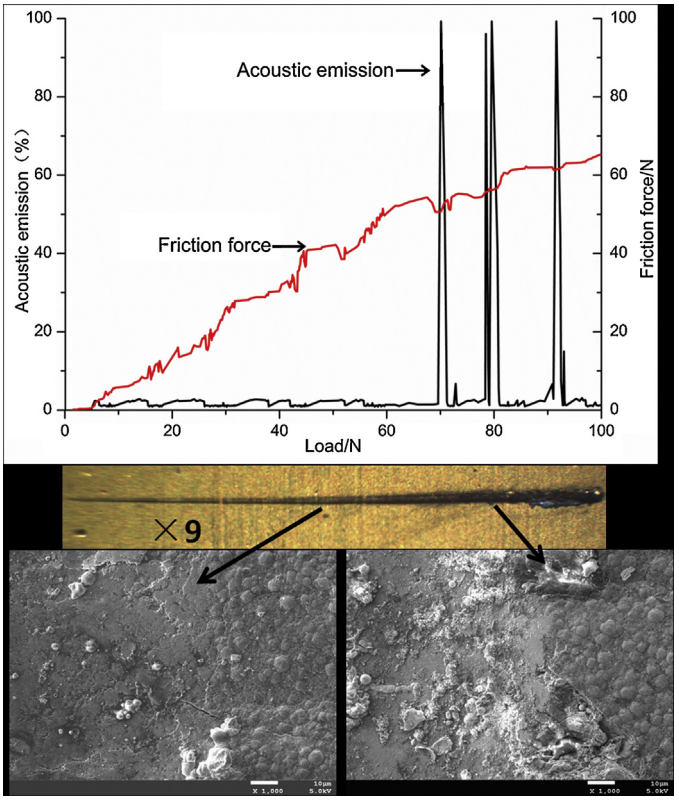

Fig. 4. Scratching curves and micrograph of the scratch track of the multilayer coating on the 35CrMo substrate.

also reduces the internal stress between the coating and substrate, and improves the interfacial bonding force of the film base. The micro-morphology of the scratch area shows that the coating in a large part of this area is damaged, and the coating at the edge of the scratches flakes off in small pieces when the critical load of 70 N is exceeded [22]. The destruction of the coating is known as flaking and cracking [23,24]. The adhesion between the remaining two high-strength steel substrates and multilayer coating is also 60 N or higher. The good adhesion also improves the corrosion resistance of the coating.

3.3. Corrosion test

The high-temperature, high-pressure, acidic environment of the gas well in the Luojiazhai Gas Field, Sichuan was simulated. The corrosion rates of the samples were determined after surface coating treatment. The corrosion rate of the unprocessed steel substrate in the hydrogen sulfide environment was also determined. The results of the corrosion weight-loss experiment are shown in Table 2.

Table 2 reveals the following observations: (1) high-strength steels have high corrosion rates (in the order of 10^{-1} mm/a) in chlorine-ion environments with high hydrogen sulfide, high

Table 2
Corrosion weight-loss results of the three coating samples.

Substrate	Processing method	Corrosion rate (mm/a)
42CrMo	Uncoated	0.5840
	Coated	0.0075
35CrMo	Uncoated	0.4223
	Coated	0.0058
40CrNiMo	Uncoated	0.3262
	Coated	0.0061

Please cite this article in press as: J. Zhang, et al., Microstructure and corrosion behavior of TiC/Ti(CN)/TiN multilayer CVD coatings on high strength steels, Appl. Surf. Sci. (2013), http://dx.doi.org/10.1016/j.apsusc.2013.05.037

Table 3
Corrosion test results of the three high-strength steel tensile test bars in the quenching state.

Substrate	Processing state	Hardness (HV)	Tensile strength (MPa)	Reduction rate of the cross-sectional area (%)
35CrMo	Coated (immersed)	2350	1670	35
	Uncoated (immersed)	411	1090	10
	Uncoated (non-immersed)	470	1600	38
42CrMo	Coating (immersed)	2410	1820	32
	Uncoated (immersed)	436	1180	15
	Uncoated (non-immersed)	509	1900	35
40CrNiMo	Coating (immersed)	2390	1690	34
	Uncoated (immersed)	399	1324	12
	Uncoated (non-immersed)	478	1700	36

temperature, and high pressure; (2) the samples processed by CVD have corrosion rates 50–70 times lower than that of the uncoated high-strength steel substrate; and (3) nickel is a good chlorine/hydrogen sulfide corrosion-resistance element [25]. With increased carbon content, the corrosion rate of the high-strength steel is accelerated, which indicates that carbon is a sensitive element for promoting the stress corrosion of the steel substrate [26,27]. The multilayer ceramic coating process almost has no selectivity for the steel substrate. Any steel substrate can substantially increase its anti-hydrogen sulfide corrosion resistance.

Micro-hardness and tensile strength tests were conducted on the three steel substrate bars that had been immersed in NACE-saturated hydrogen sulfide solution, and the test bars were processed by CVD coating. Experimental results show that the nano-hardness of the coating is not significantly reduced and maintains a high average nano-hardness of 23.3 ± 1.9 GPa (2380 HV). Table 3 compares the data of the tensile strength, the reduction of the cross-sectional area of the three high-strength steel substrates, as well as the samples processed by CVD coating before and after corrosion. The mechanical behavior trends of the steel samples before and after corrosion can also be observed in Table 3. The reduction of the cross-sectional area of the steel in tension is directly related to the yield strength characterizing the plastic deformation ability of the material. Out of the corrosion environment, the cross-sectional area of the high-strength steels has high hardness and high reduction rate even without any surface processing. However, in the case of high-chloride and high-sulfur environments, the cross-sectional areas of the high-strength steels decrease to a minimum of 10%, which may be caused by the stress corrosion. After the CVD ceramic coating growth, the three steel substrates can maintain the high reduction rate (32%) of the cross-sectional area in the high-hardness quenching state. Thus, the coating samples do not undergo plastic failure caused by stress corrosion and can maintain high hardness.

The fracture macroscopic observation and microscopic SEM morphology analysis were conducted on the coated and uncoated 35CrMo test bars in tension failure after corrosion.

Fig. 5 shows that the unprocessed sample is corroded on the surface, has a corrugated tensile part, has a flat fracture, and has no obvious necking. The unprocessed sample also shows brittle fracture morphology. The fracture morphology of the sample by SEM (Fig. 5a) shows that the particles are precipitated from the surface of the unprocessed sample; a reticular loose layer of about 0.2 mm from the outer surface exists. Magnification shows obvious etch pits with numerous cracks. The fracture area is wide and the grain boundary is destroyed with the loose deposits of grains. Fig. 5b shows the sample surfaces after corrosion testing. The surface of the uncoated sample is found to undergo severe pitting corrosion. The samples processed by CVD coating have even fractures (Fig. 6). The tensile part exhibits large necking, and susceptibility to hydrogen embrittlement is significantly reduced. The fracture morphology of the sample by SEM (Fig. 6a) shows complete coating on the surface

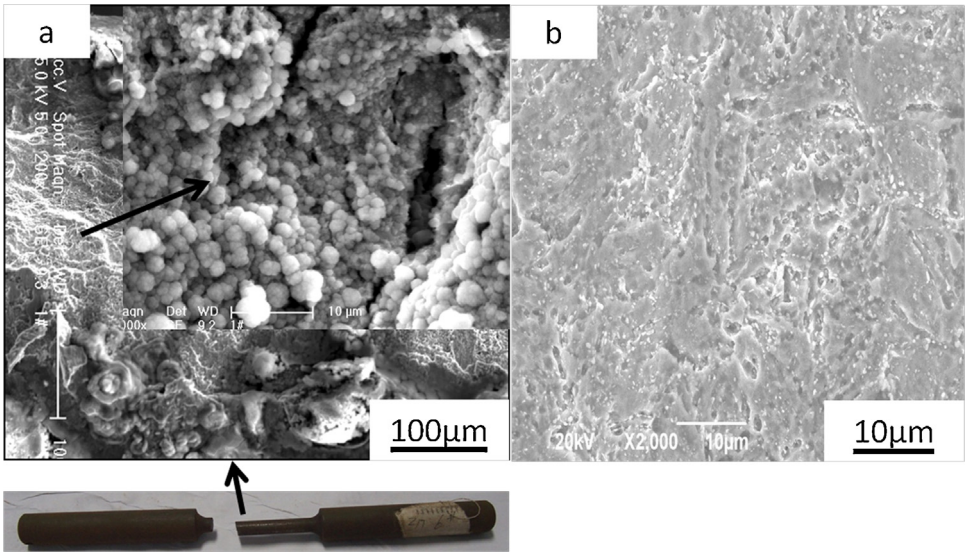

Fig. 5. SEM morphology of the uncoated specimen after an immersion corrosion test in a saturated hydrogen sulfide solution: (a) fracture morphology and (b) surface morphology.

Please cite this article in press as: J. Zhang, et al., Microstructure and corrosion behavior of TiC/Ti(CN)/TiN multilayer CVD coatings on high strength steels, Appl. Surf. Sci. (2013), http://dx.doi.org/10.1016/j.apsusc.2013.05.037

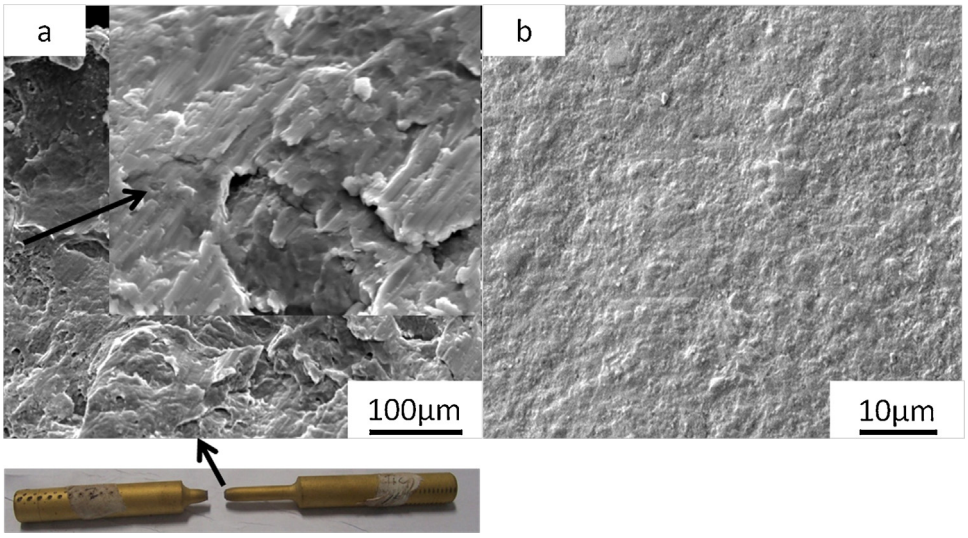

Fig. 6. SEM morphology of TiC/Ti(CN)/TiN-coated specimen after an immersion corrosion test in saturated hydrogen sulfide solution: (a) fracture morphology and (b) surface morphology.

of the samples as well as the internal integrity of the steel substrate without the loose layer and the corrosion crack. The surface of the CVD coated sample is smooth and has no corrosion pits or cracks (Fig. 6b). This finding indicates that the TiC/Ti(CN)/TiN multilayer coatings can act as barrier layers and effectively prevent the diffusion and penetration of hydrogen atoms into steel substrate [13,14,28].

Fig. 7 shows the XRD pattern of the 35CrMo substrate and the samples processed by the CVD coating after an immersion corrosion test in saturated hydrogen sulfide solution. The XRD pattern shows the characteristic peaks of Fe(Cr) substitution solid solution and FeS in the steel substrate corrosion phase. Thus, the surface of the steel substrate undergoes the $Fe + H_2S \rightarrow FeS + H_2$ reaction because of the effect of hydrogen sulfide. In other words, hydrogen precipitation occurs when generating FeS, which is the main reason for the hydrogen-induced stress corrosion damage to the high-strength steels [29,30]. Fig. 8 shows the XRD pattern of the samples processed by CVD after corrosion. After the same corrosion test, the coating samples do not show any corrosion product, and the surface remains as TiC/Ti($C_{0.3}N_{0.7}$)/TiN multilayer coatings. The multilayer

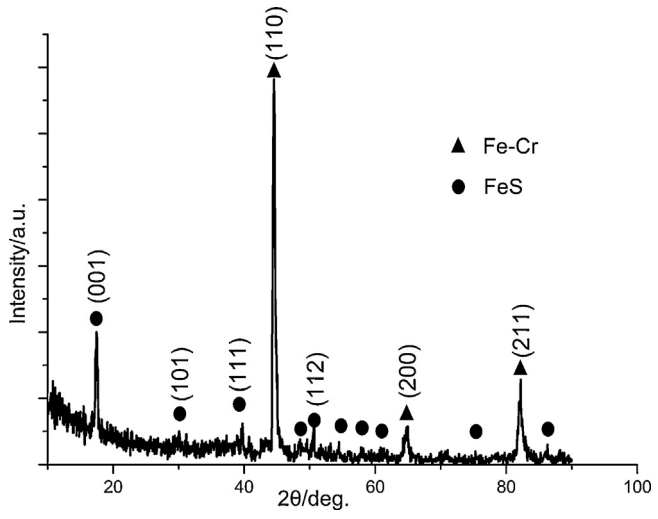

Fig. 7. XRD pattern of the uncoated specimen after an immersion corrosion test in saturated hydrogen sulfide solution.

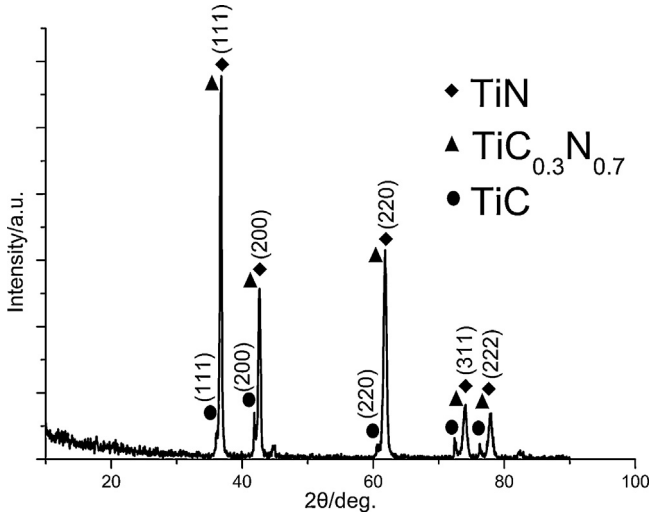

Fig. 8. XRD pattern of the TiC/Ti(CN)/TiN-coated specimen after an immersion corrosion test in saturated hydrogen sulfide solution.

coatings deposited by CVD are uniform, dense, and closely integrated with the substrates. Thus, few spaces and defects appear in the coatings. The existence of the multilayer interface structure can reduce the internal stress of the film, thereby preventing cracks and inhibiting the formation of penetrative pinholes, which are harmful to corrosion. The hydrogen barrier effectively prevents the hydrogen-induced stress-corrosion cracking caused by the diffusion and permeation of the hydrogen atoms to the direction of the substrate.

In summary, the surface deposition of TiC/Ti(CN)/TiN multilayer coatings can greatly improve the resistance of the three high-strength steels to chloride-ion corrosion and hydrogen sulfide stress corrosion, and can satisfy the requirements of the exploration of complex oil and gas fields with a corrosive environment.

4. Conclusion

(1) The CVD method can be used to prepare uniform and dense TiC/Ti(CN)/TiN multilayer coatings, which have high hardness and high adhesion, on the surface of three high-strength steel substrates.

Please cite this article in press as: J. Zhang, et al., Microstructure and corrosion behavior of TiC/Ti(CN)/TiN multilayer CVD coatings on high strength steels, Appl. Surf. Sci. (2013), http://dx.doi.org/10.1016/j.apsusc.2013.05.037

(2) Compared with the high-strength steel substrate, the coated steel substrate sample has good resistance to chloride-ion corrosion. In particular, the high-strength steel substrate strongly promotes the resistance to hydrogen sulfide stress corrosion cracking. After corrosion, the coating maintains high hardness and can be used for the surface protection of high-strength steels in complex hydrogen sulfide corrosion environments.

References

[1] B. Beidokhti, A. Dolati, A.H. Koukabi, Effects of alloying elements and microstructure on the susceptibility of the welded HSLA steel to hydrogen-induced cracking and sulfide stress cracking, Materials Science and Engineering A 507 (2009) 167–173.
[2] M. Al-Mansour, A.M. Alfantazi, M. El-Boujdaini, Sulfide stress cracking resistance of API-X100 high strength low alloy steel, Materials and Design 30 (2009) 4088–4094.
[3] M. Christophe, S. Thomas, Composition optimization of high-strength steels for sulfide stress cracking resistance improvement, Corrosion Science 51 (2009) 2878–2884.
[4] NACE TM-0177 Standard Test Method. Laboratory Testing of Metals for Resistance to Sulfide Stress Cracking and Stress Corrosion Cracking in H_2S Environments, NACE International, Houston, 2005.
[5] P. Fassina, F. Bolzoni, G. Fumagalli, L. Lazzari, L. Vergani, A. Sciuccati, Influence of hydrogen and low temperature on mechanical behavior of two pipeline steels, Engineering Fracture Mechanics 81 (2012) 43–55.
[6] Y.S. Tian, C.Z. Chen, S.T. Li, Q.H. Huo, Research process on laser surface modification of titanium alloys, Applied Surface Science 242 (2005) 177–184.
[7] B.G. Guo, J.S. Zhou, S.T. Zhang, H.D. Zhou, Y.P. Pu, J.M. Chen, Microstructure and tribological properties of in situ synthesized TiN/Ti_3Al intermetallic matrix composite coatings on titanium by laser cladding and laser nitriding, Materials Science and Engineering A 480 (2008) 404–410.
[8] D.M. Devia, E.R. Parra, P.J. Arango, Comparative study of titanium carbide and nitride coatings grown by cathodic vacuum arc technique, Applied Surface Science 258 (2011) 1164–1174.
[9] Q.Z. Wang, F. Zhou, K.M. Chen, M.L. Wang, T. Qian, Friction and wear properties of TiCN coatings sliding against SiC and steel balls in air and water, Thin Solid Films 519 (2011) 4830–4841.
[10] L. Chen, S.Q. Wang, Y. Du, J. Li, Microstructure and mechanical properties of gradient Ti(C, N) and TiN/Ti(C, N) multilayer PVD coatings, Materials Science and Engineering A 478 (2008) 336–339.
[11] X.M. Li, Y. Han, Mechanical properties of Ti($C_{0.7}N_{0.3}$) film produced by plasma electrolytic carbonitriding of Ti6Al4V alloy, Applied Surface Science 254 (2008) 6350–6357.
[12] S.W. Huang, M.W. Ng, M. Samandi, M. Brandt, Tribological behavior and microstructure of $TiC_XN_{(1-X)}$ coatings deposited by filtered arc, Wear 252 (2002) 566–579.
[13] C.Q. Shan, A.J. Wu, Q.W. Chen, The behavior of diffusion and permeation of tritium through 316L stainless steel, Journal of Nuclear Materials 179–181 (1991) 322–324.
[14] C.Q. Shan, A.J. Wu, Y.J. Li, Z.Q. Zhao, Q.W. Chen, Q.R. Huang, S.L. Shi, The behavior of diffusion and permeation of tritium through 316L stainless steel with coating of TiC and TiN + TiC, Journal of Nuclear Materials 191–194 (1992) 221–226.
[15] H.A. Jehn, Multicomponent and multiphase hard coatings for tribological applications, Surface and Coatings Technology 131 (2000) 433–440.
[16] L.A. Dobrzanski, W. Kwasny, Z. Brytan, R. Shishkov, B. Tomov, Structure and properties of the Ti + Ti(C, N) coatings obtained in the PVD process on sintered high speed steel, Journal of Materials Processing Technology 157–158 (2004) 312–316.
[17] C. Liu, A. Leyland, Q. Bi, A. Matthews, Corrosion resistance of multi-layered plasma-assisted physical vapour deposition TiN and CrN coatings, Surface and Coatings Technology 141 (2001) 164–173.
[18] C.F. Cai, Z.Y. Xie, R.H. Worden, G.Y. Hu, L.S. Wang, H. He, Methane-dominated thermochemical sulphate reduction in the Triassic Feixianguan Formation East Sichuan Basin, China: towards prediction of fatal H_2S concentrations, Marine and Petroleum Geology 21 (2004) 1265–1279.
[19] Z.X. Guo, J. Xiong, M. Yang, S.J. Xiong, J.Z. Chen, S.Q. Bi, Characterization and properties of MTCVD Ti(C, N) coated cemented carbide substrates with Fe/Ni binder, International Journal of Refractory Metals & Hard Materials 28 (2010) 238–242.
[20] J. Smolik, K. Zdunek, B. Larisch, Investigation of adhesion between component layers of a multi-layer coating TiC/Ti(C_X, N_{1-X})/TiN by the scratch-test method, Vacuum 55 (1999) 45–50.
[21] W. Tang, K.W. Xu, P. Wang, X. Li, Scratch behavior of multi-layered metallic thin films on Al_2O_3 substrates, Surface and Coatings Technology 182 (2004) 143–148.
[22] F. Attar, T. Johannesson, Adhesion evaluation of thin ceramic coatings on tool steel using the scratch testing technique, Surface and Coatings Technology 78 (1996) 87–102.
[23] B. Hammer, A.J. Perry, P. Laeng, P.A. Steinmann, The scratch test adhesion of TiC deposited industrially by chemical vapour deposition on steel, Thin Solid Films 96 (1982) 45–51.
[24] L.A. Dobrzanski, M. Adamiak, Structure and properties of the TiN and Ti(C, N) coatings deposited in the PVD process on high-speed steels, Journal of Materials Processing Technology 133 (2003) 50–62.
[25] X.H. Zhao, Y. Han, Z.Q. Bai, B. Wei, The experiment research of corrosion behavior about Ni-based alloys in stimulant solution containing H_2S/CO_2, Electrochimica Acta 56 (2011) 7725–7731.
[26] NACE MR-0103 Standard Practice. Materials Resistance to Sulfide Stress Cracking in Corrosive Petroleum Refining Environments, NACE International, Houston, 2010.
[27] A. Cigada, T. Pastore, P. Pedeferri, B. Vicentini, The sulfide stress corrosion cracking of high alloy stainless steels for oil and natural gas wells, Corrosion Science 27 (1987) 1213–1223.
[28] Z.Y. Yao, J.K. Hao, C.S. Zhou, C.Q. Shan, J.N. Yu, The permeation of tritium through 316L stainless steel with multiple coatings, Journal of Nuclear Materials 283–287 (2000) 1287–1291.
[29] D. Delafosse, T. Magnin, Hydrogen induced plasticity in stress corrosion cracking of engineering systems, Engineering Fracture Mechanics 68 (2001) 693–729.
[30] J. Woodtil, R. Kieselbach, Damage due to hydrogen embrittlement and stress corrosion cracking, Engineering Failure Analysis 7 (2000) 427–450.

Please cite this article in press as: J. Zhang, et al., Microstructure and corrosion behavior of TiC/Ti(CN)/TiN multilayer CVD coatings on high strength steels, Appl. Surf. Sci. (2013), http://dx.doi.org/10.1016/j.apsusc.2013.05.037